

TOP-YUKAWA-INDUCED CORRECTIONS TO HIGGS PAIR PRODUCTION

MARGARETE MÜHLLEITNER¹, JOHANNES SCHLENK² AND MICHAEL SPIRA²¹ *Institut für Theoretische Physik, KIT, D-76128 Karlsruhe, Germany*² *Paul Scherrer Institut, CH-5232 Villigen PSI, Switzerland***Abstract**

Higgs-boson pair production at hadron colliders is dominantly mediated by the loop-induced gluon-fusion process $gg \rightarrow HH$ that is generated by heavy top loops within the Standard Model with a minor per-cent level contamination of bottom-loop contributions. The QCD corrections turn out to be large for this process. In this note, we derive the top-Yukawa-induced part of the electroweak corrections to this process and discuss their relation to an effective trilinear Higgs coupling with integrated out top-quark contributions.

1 Introduction

The discovery of a bosonic particle with a mass of (125.09 ± 0.24) GeV [1] turned out to be in agreement with the Standard-Model (SM) Higgs boson within the present uncertainties of all production and decay modes. Its coupling strengths to SM gauge bosons, i.e. ZZ, W^+W^- , and fermion pairs as τ, μ leptons and bottom quarks as well as the loop-induced couplings to gluon and photon pairs, have been measured with accuracies of 10 – 50%. All measurements are in agreement with the SM predictions within their uncertainties [2]. In addition, there are very strong indications that the newly discovered boson carries zero spin and positive CP-parity, i.e. possible deviations from these hypotheses are strongly constrained by the accuracy of present experimental data. Thus, there is increasing evidence that this particle is indeed the long-sought SM Higgs boson. Its discovery is of vital importance for the consistency of the SM and the success of the predictions for the precision electroweak observables which are in striking agreement with measurements at LEP and SLC [3]. The discovery of a SM-like Higgs boson at the LHC completed the SM of electroweak and strong interactions. The existence of the Higgs boson is inherently related to the mechanism of spontaneous symmetry breaking while preserving the full gauge symmetry and the renormalizability of the SM [4], since the Higgs boson permits the SM particles to be weakly interacting up to high-energy scales [5]. However, with the knowledge of the Higgs-boson mass all its properties within the SM are uniquely fixed, i.e. the SM does not allow the Higgs couplings to the SM particles to deviate from their unique predictions.

The minimal model as realized in the SM requires the introduction of one isospin doublet of Higgs fields that leads after spontaneous symmetry breaking to the existence of one scalar Higgs boson. A crucial experimental goal is the measurement of the Higgs potential, since the formation of a non-trivial ground state with a finite vacuum expectation value of the Higgs field causes electroweak symmetry breaking so that the experimental verification of the Higgs potential itself is of highest interest. The parameters describing the Higgs potential

are the Higgs mass and self-interactions of the Higgs field. The production of Higgs-boson pairs is the first class of processes that offers the direct access to the trilinear self-coupling of the Higgs boson as a first step towards the reconstruction of the full Higgs potential. At the Large Hadron Collider (LHC), the dominant Higgs-boson pair production mechanism is provided by the gluon-fusion process $gg \rightarrow HH$, while the other production modes as vector-boson fusion (VBF) $qq \rightarrow qqHH$, double Higgs-strahlung $q\bar{q} \rightarrow W/Z + HH$ and double Higgs bremsstrahlung off top quarks $q\bar{q}, gg \rightarrow t\bar{t}HH$ are suppressed by at least one order of magnitude [6]. The individual production cross sections roughly follow the pattern of single-Higgs boson production but are in general smaller by about three orders of magnitude. Since the trilinear Higgs coupling contributes only to a subset of diagrams of each production process the sensitivity to the trilinear Higgs coupling is reduced due to the dominance of the continuum diagrams. The slope of the gluon-fusion cross section as a function of the trilinear Higgs coupling λ follows the rough behaviour $\Delta\sigma/\sigma \sim -\Delta\lambda/\lambda$ around the SM prediction [6–8]. This implies that the uncertainties of the production cross section are immediately translated to the uncertainties of the extracted trilinear self-coupling so that the reduction of the theoretical uncertainties of the Higgs pair production cross section is crucial for an accurate extraction of the trilinear self-interaction from the experimental measurements. This feature translates to a similar situation for the distributions as well. The trilinear coupling develops a significant contribution for Higgs-pair production closer to the production threshold, while it dies out for large invariant Higgs-pair masses. In the last range, however, statistics will be small in experiment so that the bulk of reconstructed events will emerge from the region closer to the threshold.

The gluon-fusion mechanism $gg \rightarrow HH$ is mediated by top- and to a much lesser extent bottom-quark loops, see Fig. 1. The full next-to-leading-order (NLO) QCD corrections have been calculated by a time-consuming numerical integration of the corresponding two-loop integrals, since there are no systematic analytical methods to calculate the corresponding two-loop integrals [9, 10]. Similar to the single-Higgs case they enhance the cross section by about 100%. Because the invariant mass of the final-state Higgs-boson pair is significantly larger than in the single-Higgs case, the heavy top-quark limit (HTL) works less reliably for Higgs-boson pairs. The full NLO QCD corrections result in a decrease of the total cross section by about 15%, due to finite NLO top mass effects beyond the heavy-top limit, at the LHC for a c.m. energy of 14 TeV. This shows that the heavy-top limit for the relative QCD corrections [7] works still quite well for the total cross section also in the Higgs-pair case. For the exclusive cross section at large invariant Higgs-pair masses, however, the finite mass effects at NLO can reach a level of -30% . The next-to-NLO (NNLO) QCD corrections to the total cross section have been obtained in the heavy top-quark limit. They imply an additional moderate rise of the total cross section by about 20% [11]. Recently, the next-to-NNLO (N³LO) QCD corrections to the total cross section became available and turned out to be small, affecting the total cross section at the few per-cent level only [12]. NNLO top mass effects have been estimated to about 5% by means of a heavy top-quark expansion of the 2-loop virtual corrections [13]. Beyond NNLO, the next-to-next-to-leading-logarithmic (NNLL) soft and collinear gluon resummation contributes 5–10% to the total cross section [14]. The factorization and renormalization scale dependence has been reduced to about

5%. In order to obtain an estimate of the residual theoretical uncertainties, however, the uncertainties due to the scheme and scale choice of the virtual top mass have to be taken into account as well. These latter effects increase the theoretical uncertainties to a level of 20–25% [10]. The electroweak corrections to this process are unknown. They are expected in the 10%-range for the total cross section, but larger in the tails of the distributions.

In this work we investigate the electroweak corrections induced by the top-Yukawa coupling as a uniquely defined contribution to the full electroweak corrections. In Section 2, we will define our notation and the corresponding leading-order (LO) result for $gg \rightarrow HH$. In Section 3, we describe the effective Higgs (pair) couplings to gluons in the HTL and the effective trilinear Higgs coupling within the effective-potential approach, where the top contributions are integrated out. Section 4 describes the NLO calculation and Section 5 our results with a discussion of our findings. In Section 6, we conclude.

2 Higgs-boson pair production at leading order

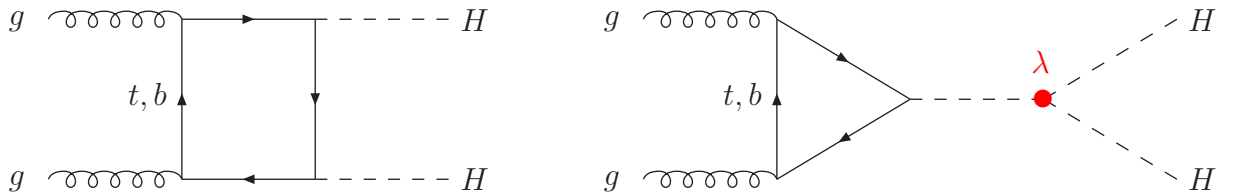


Figure 1: *Diagrams contributing to Higgs-boson pair production via gluon fusion. The contribution of the trilinear Higgs coupling is marked in red.*

The LO Higgs pair production via gluon fusion is mediated by heavy top-loop contributions and a marginal contribution of bottom loops, see Fig. 1. In this work we neglect the bottom-loop contributions and take into account the top loops only. The Higgs-boson pair production cross section at LO is given by

$$\sigma_{\text{LO}} = \int_{\tau_0}^1 d\tau \frac{d\mathcal{L}^{gg}}{d\tau} \hat{\sigma}_{\text{LO}}(Q^2 = \tau s), \quad (1)$$

where \mathcal{L}^{gg} denotes the gluonic parton luminosity given in terms of the gluon densities $g(x, \mu_F)$,

$$\frac{d\mathcal{L}^{gg}}{d\tau} = \int_{\tau}^1 \frac{dx}{x} g(x, \mu_F) g\left(\frac{\tau}{x}, \mu_F\right) \quad (2)$$

at the factorization scale μ_F , and the integration boundary is given by $\tau_0 = 4M_H^2/s$, where s denotes the hadronic center-of-mass (c.m.) energy squared and M_H the Higgs mass. The scale $Q^2 = M_{HH}^2$ is defined in terms of the invariant mass M_{HH} of the Higgs pair at LO.

The LO partonic cross section can be cast into the form

$$\hat{\sigma}_{LO} = \frac{G_F^2 \alpha_s^2(\mu_R)}{512(2\pi)^3} \int_{\hat{t}_-}^{\hat{t}_+} d\hat{t} \left[|C_\Delta F_\Delta + F_\square|^2 + |G_\square|^2 \right], \quad (3)$$

where the integration boundaries are given by

$$\hat{t}_\pm = -\frac{1}{2} \left[Q^2 - 2M_H^2 \mp Q^2 \sqrt{1 - 4\frac{M_H^2}{Q^2}} \right], \quad (4)$$

and the symmetry factor 1/2 for the identical Higgs bosons in the final state is included. The coefficient $C_\Delta = \lambda_{HHH}v/(Q^2 - M_H^2)$ involves the trilinear Higgs coupling that is related to the Higgs mass and the vacuum expectation value (vev) v at LO,

$$\lambda_{HHH} = 3\frac{M_H^2}{v}, \quad (5)$$

where the vev is related to the Fermi constant $G_F = 1/(\sqrt{2}v^2)$. The factor $\alpha_s(\mu_R)$ denotes the strong coupling at the renormalization scale μ_R . The form factors F_Δ of the LO triangle diagrams and F_\square, G_\square of the LO box diagrams can be found in Refs. [15]. In the HTL they approach simple expressions, $F_\Delta \rightarrow 2/3$, $F_\square \rightarrow -2/3$ and $G_\square \rightarrow 0$.

3 Effective Lagrangians

In this section we address the effective gluonic single- and double-Higgs couplings as well as the effective Higgs self-couplings after integrating out the heavy-top contributions, i.e. the effective couplings valid in the HTL at the leading order of an inverse large top-mass expansion.

3.1 Gluonic Higgs couplings

In the HTL, the top-Yukawa-induced electroweak corrections to the effective Hgg and $HHgg$ couplings can be obtained as

$$\mathcal{L}_{eff} = C_1 \frac{\alpha_s}{12\pi} G^{a\mu\nu} G_{\mu\nu}^a \log \left(1 + C_2 \frac{H}{v} \right), \quad (6)$$

where $G_{\mu\nu}^a$ denotes the gluonic field-strength tensor and H the SM Higgs field. The radiatively corrected coefficients are given by

$$\begin{aligned} C_1 &= 1 - 3x_t + \mathcal{O}(x_t^2) \\ C_2 &= 1 + \frac{7}{2}x_t + \mathcal{O}(x_t^2), \end{aligned} \quad (7)$$

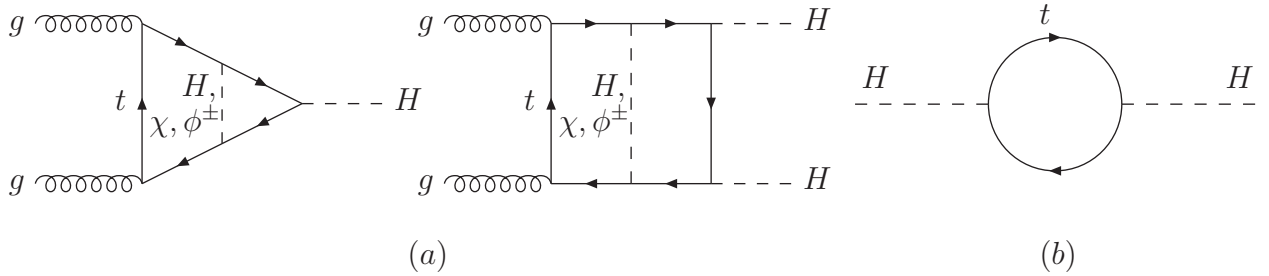


Figure 2: *Typical diagrams contributing to the top-Yukawa-induced electroweak corrections to the effective Lagrangian: (a) vertex corrections, (b) wave-function corrections. The fields χ, ϕ^\pm denote the pseudoscalar and charged would-be Goldstones.*

with $x_t = G_F m_t^2 / (8\sqrt{2}\pi^2)$, where C_1 describes the genuine corrections to the Hgg and $HHgg$ vertices [16] (see Fig. 2a) and C_2 the universal top-Yukawa-induced correction related to the Higgs wave-function and vacuum expectation value [17] (see Fig. 2b). This yields the explicit effective Hgg and $HHgg$ couplings,

$$\mathcal{L}_{eff} = \frac{\alpha_s}{12\pi} G^{a\mu\nu} G_{\mu\nu}^a \left\{ (1 + \delta_1) \frac{H}{v} + (1 + \eta_1) \frac{H^2}{2v^2} + \mathcal{O}(H^3) \right\} \quad (8)$$

where

$$\delta_1 = \frac{x_t}{2} + \mathcal{O}(x_t^2), \quad \eta_1 = 4x_t + \mathcal{O}(x_t^2). \quad (9)$$

This effective Lagrangian describes the electroweak corrections induced by x_t to the Hgg and $HHgg$ vertices in the HTL and will be used in this limit in the following. We would like to point out explicitly that the square root of the wave-function counterterm of the external Higgs boson(s) is already taken into account in this effective Lagrangian.

3.2 Higgs self-couplings

The starting point of effective Higgs self-couplings is the effective one-loop corrected Higgs potential involving virtual top-quark effects of the SM [18],

$$\begin{aligned} V_{eff} &= V_0 + V_1 \\ V_0 &= \mu_0^2 |\phi|^2 + \frac{\lambda_0}{2} |\phi|^4 \\ V_1 &= \frac{3\overline{m}_t^4}{16\pi^2} C_\epsilon \left(\frac{1}{\epsilon} + \log \frac{\overline{\mu}^2}{\overline{m}_t^2} + \frac{3}{2} \right), \end{aligned} \quad (10)$$

with the bare Higgs self-coupling λ_0 , the SM Higgs doublet in unitary gauge,

$$\phi = \frac{1}{\sqrt{2}} \begin{pmatrix} 0 \\ v + H \end{pmatrix} \quad (11)$$

the loop coefficient

$$C_\epsilon = \Gamma(1 + \epsilon)(4\pi^2)^\epsilon \quad (12)$$

and the field-dependent top-mass parameter

$$\bar{m}_t = m_t \left(1 + \frac{H}{v} \right). \quad (13)$$

The expression above for the effective Higgs potential involves the 't Hooft scale $\bar{\mu}$. After minimization of the effective Higgs potential by the tadpole equation,

$$\begin{aligned} \mu_0^2 &= -\frac{\lambda_0}{2}v^2 + \delta\mu^2 \\ \delta\mu^2 &= -\frac{3m_t^4}{4\pi^2v^2}C_\epsilon \left\{ \frac{1}{\epsilon} + \log \frac{\bar{\mu}^2}{m_t^2} + 1 \right\} \end{aligned} \quad (14)$$

and the renormalization of the Higgs mass,

$$\begin{aligned} M_{H0}^2 &= \lambda_0v^2 = \lambda v^2 + (\delta\lambda)v^2 = \lambda v^2 + \delta M_H^2 \\ \delta M_H^2 &= -\frac{3m_t^4}{2\pi^2v^2}C_\epsilon \left\{ \frac{1}{\epsilon} + \log \frac{\bar{\mu}^2}{m_t^2} \right\}, \end{aligned} \quad (15)$$

the effective Higgs trilinear (quartic) self-coupling can be obtained by the third (fourth) derivative of this effective Higgs potential with respect to the physical Higgs field H ,

$$\lambda_{HHH}^{eff} = 3\frac{M_H^2}{v} + \Delta\lambda_{HHH}, \quad \lambda_{HHHH}^{eff} = 3\frac{M_H^2}{v^2} + \Delta\lambda_{HHHH}, \quad (16)$$

with

$$\Delta\lambda_{HHH} = -\frac{3m_t^4}{\pi^2v^3}, \quad \Delta\lambda_{HHHH} = -\frac{12m_t^4}{\pi^2v^4}. \quad (17)$$

These effective NLO couplings are the relevant Higgs self-interactions in the HTL and will be compared with the full triple-vertex corrections within this work.

4 Top-Yukawa-induced electroweak corrections to Higgs pair production

The top-Yukawa-induced electroweak corrections arise from NLO diagrams involving top-quark loops as shown in Fig. 3, where the tadpole diagrams are displayed explicitly. For simplicity, we will use the relative corrections of Eq. (8) to the ggH and $ggHH$ vertices in the HTL, while the radiative corrections to the triple-Higgs vertex and Higgs self-energies are treated with full top-mass dependence. Since there are no real corrections at the NLO

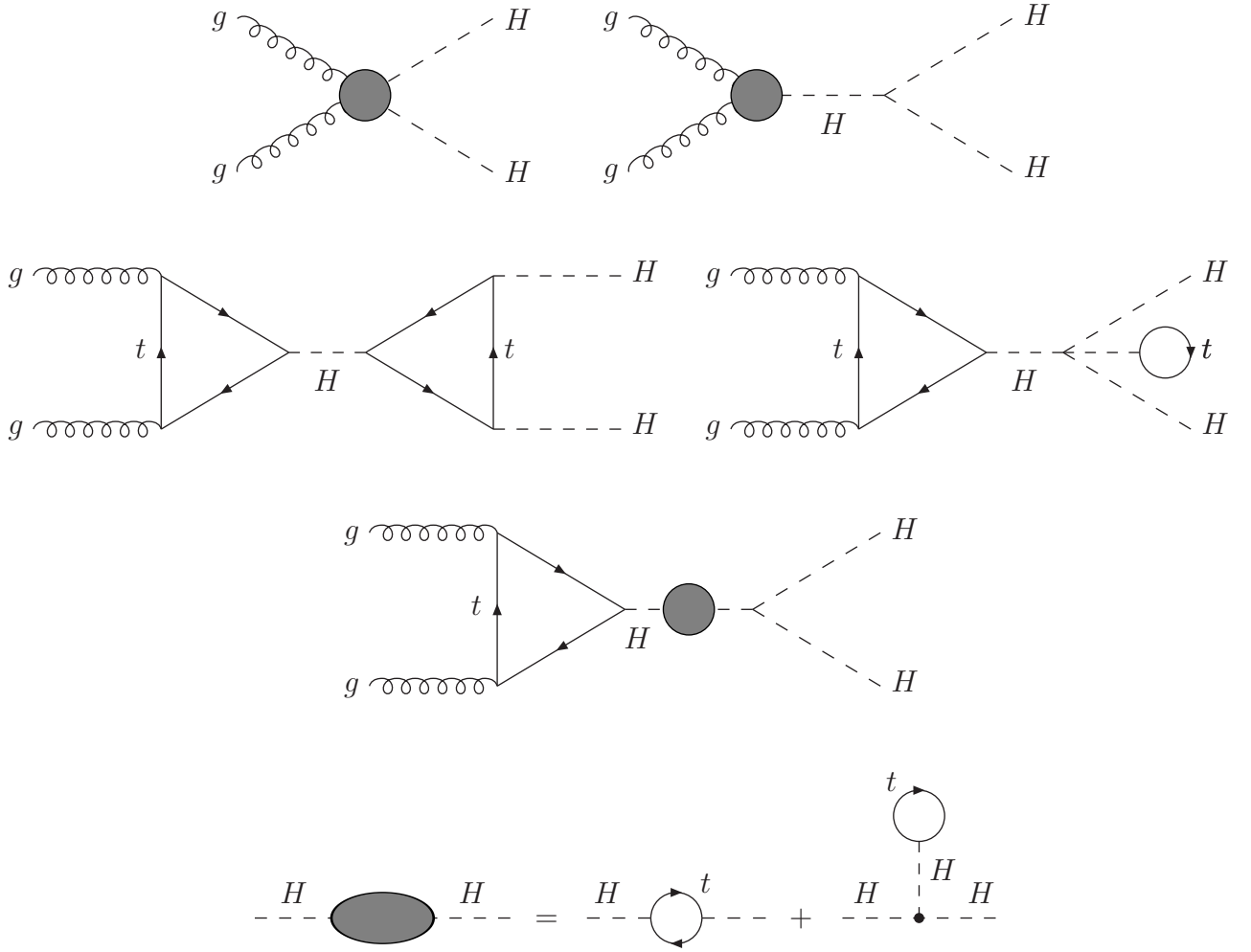


Figure 3: *Generic diagrams describing the top-Yukawa-induced electroweak corrections to Higgs-boson pair production via gluon fusion. The blobs of the first two diagrams are determined by the effective Lagrangian of Eq. (8) in the HTL.*

electroweak level, the radiative corrections can be implemented by a shift of the LO form factors of Eq. (3),

$$\begin{aligned} C_{\Delta}F_{\Delta} &\rightarrow C_{\Delta}F_{\Delta}(1 + \Delta_{\Delta}) \\ F_{\square} &\rightarrow F_{\square}(1 + \Delta_{\square}), \end{aligned} \quad (18)$$

while the LO form factor G_{\square} does not receive top-Yukawa-induced electroweak corrections in our approach, since G_{\square} vanishes in the HTL. The top-Yukawa-induced radiative corrections in Eq. (18) read as

$$\begin{aligned} \Delta_{\Delta} &= \delta_1 + \Delta_{HHH} \\ \Delta_{\square} &= \eta_1, \end{aligned} \quad (19)$$

where the vertex, self-energy and counterterm corrections are given by

$$\begin{aligned}
\Delta_{HHH} &= \Delta_{vertex} + \Delta_{self} + \Delta_{CT} \\
\Delta_{vertex} &= \frac{m_t^4}{v^2 M_H^2} \frac{8}{(4\pi)^2} \left\{ B_0(Q^2; m_t, m_t) + 2B_0(M_H^2; m_t, m_t) \right. \\
&\quad \left. + \left(4m_t^2 - \frac{Q^2 + 2M_H^2}{2} \right) C_0(Q^2, M_H^2, M_H^2; m_t, m_t, m_t) \right\} + \frac{T_1}{v M_H^2} \\
\Delta_{self} &= \frac{\Sigma_H(Q^2)}{Q^2 - M_H^2} + \frac{1}{2} \Sigma'_H(M_H^2) \\
\Delta_{CT} &= \frac{\delta M_H^2}{Q^2 - M_H^2} + \frac{\delta \lambda_{HHH}}{\lambda_{HHH}}. \tag{20}
\end{aligned}$$

We are adopting the scalar integrals in $n = 4 - 2\epsilon$ dimensions,

$$\begin{aligned}
A_0(m) &= \frac{(4\pi)^2}{i} \bar{\mu}^{4-n} \int \frac{d^n k}{(2\pi)^n} \frac{1}{k^2 - m^2} \\
B_0(p^2; m_1, m_2) &= \frac{(4\pi)^2}{i} \bar{\mu}^{4-n} \int \frac{d^n k}{(2\pi)^n} \frac{1}{(k^2 - m_1^2)[(k+p)^2 - m_2^2]} \\
B'_0(p^2; m_1, m_2) &= \frac{\partial}{\partial p^2} B_0(p^2; m_1, m_2) \\
C_0(p_1^2, p_2^2, (p_1 + p_2)^2; m_1, m_2, m_3) &= \frac{(4\pi)^2}{i} \bar{\mu}^{4-n} \int \frac{d^n k}{(2\pi)^n} \frac{1}{(k^2 - m_1^2)[(k+p_1)^2 - m_2^2]} \\
&\quad \times \frac{1}{[(k+p_1+p_2)^2 - m_3^2]}. \tag{21}
\end{aligned}$$

In the expression of Eq. (20), the self-energy $\Sigma_H(Q^2)$ and its derivative $\Sigma'_H(Q^2)$, the tadpole term T_1/v , the trilinear Higgs-coupling counterterm $\delta \lambda_{HHH}$ and the Higgs-mass counterterm δM_H^2 are given by

$$\begin{aligned}
\Sigma_H(Q^2) &= 3 \frac{T_1}{v} + 6 \frac{m_t^2}{(4\pi)^2 v^2} \left\{ 2A_0(m_t) + (4m_t^2 - Q^2) B_0(Q^2; m_t, m_t) \right\} + \mathcal{O}(m_t^0) \\
\Sigma'_H(Q^2) &= 6 \frac{m_t^2}{(4\pi)^2 v^2} \left\{ (4m_t^2 - Q^2) B'_0(Q^2; m_t, m_t) - B_0(Q^2; m_t, m_t) \right\} + \mathcal{O}(m_t^0) \\
\frac{T_1}{v} &= -12 \frac{m_t^2}{(4\pi)^2 v^2} A_0(m_t) \\
\frac{\delta \lambda_{HHH}}{\lambda_{HHH}} &= \frac{\delta M_H^2}{M_H^2} + \frac{1}{2} \frac{\Sigma_W(0)}{M_W^2} \\
\frac{\Sigma_W(0)}{M_W^2} &= 2 \frac{T_1}{v M_H^2} + \frac{2m_t^2}{(4\pi)^2 v^2} \left\{ B_0(0; m_t, 0) + 2B_0(0; m_t, m_t) + m_t^2 B'_0(0; m_t, 0) \right\} + \mathcal{O}(m_t^0) \\
\delta M_H^2 &= -\Sigma_H(M_H^2), \tag{22}
\end{aligned}$$

where the self-energies Σ_H, Σ_W and the Higgs-mass counterterm include tadpole contributions as well, and we only kept terms of $\mathcal{O}(m_t^4)$ and $\mathcal{O}(m_t^2)$ for the counterterms to be

consistent. For the calculation, we have used the alternative tadpole-scheme of Ref. [19]¹ and implemented the electroweak parameters in the G_F scheme, i.e. choosing G_F, M_Z, M_W as input parameters for the electroweak gauge sector, while the Weinberg angle θ_W and the QED coupling α are derived quantities. In addition, we have taken into account that the effective Lagrangian of Eq. (8) contains the wave-function renormalization of the external Higgs fields that has to be compensated in the corrections Δ_{HHH} to avoid double counting. Within our electroweak renormalization, the trilinear coupling is given by its LO expression in terms of the renormalized Higgs mass and vacuum expectation value of Eq. (5). We will compare the explicit NLO result of Eq. (18) to the corresponding one using the effective trilinear coupling λ_{HHH}^{eff} , i.e. adding the corresponding matching term

$$\begin{aligned}\Delta_{HHH} &\rightarrow \Delta_{HHH} + \Delta_\lambda \\ \Delta_\lambda &= -\frac{\Delta\lambda_{HHH}}{\lambda_{HHH}} = 16\frac{m_t^4}{(4\pi)^2 v^2 M_H^2}\end{aligned}\quad (23)$$

with $\Delta\lambda_{HHH}$ of Eq. (17) to avoid double counting and using the effective coupling $\lambda_{HHH} \rightarrow \lambda_{HHH}^{eff}$ of Eq. (16) for the triangle coefficient C_Δ in Eq. (3) in both the LO and NLO expressions.

The relative electroweak corrections to the Higgs-pair production cross section are defined by expanding the expression of Eq. (3) up to NLO by using the corrected form factors of Eq. (18) at the parton level,

$$\begin{aligned}\hat{\sigma}_{NLO} &= \hat{\sigma}_{LO} + \Delta\hat{\sigma} \\ \Delta\hat{\sigma} &= \frac{G_F^2 \alpha_s^2(\mu_R)}{512(2\pi)^3} \int_{\hat{t}_-}^{\hat{t}_+} d\hat{t} \, 2\Re \left\{ (C_\Delta F_\Delta + F_\square)^* (C_\Delta F_\Delta \Delta_\Delta + F_\square \Delta_\square) \right\}\end{aligned}\quad (24)$$

such that the hadronic cross section is corrected as

$$\begin{aligned}\sigma_{NLO} &= \sigma_{LO} (1 + \delta_{elw}) \\ \delta_{elw} &= \frac{\Delta\sigma}{\sigma_{LO}} \\ \Delta\sigma &= \int_{\tau_0}^1 \frac{\mathcal{L}^{gg}}{d\tau} \Delta\hat{\sigma}\end{aligned}\quad (25)$$

Within this expression we will either use the LO expression of the triple Higgs coupling λ_{HHH} of Eq. (5) or the radiatively-corrected effective coupling λ_{HHH}^{eff} of Eq. (16) with the according form of the radiative corrections as shown in Eq. (23).

5 Results

For our numerical analysis we work at a c.m. energy of 14 TeV at the LHC and use a top pole mass of $m_t = 172.5$ GeV according to the conventions of the LHC Higgs Working Group

¹We have checked explicitly that in the conventional approach of using a tadpole counterterm to cancel all tadpole diagrams, we arrive at the same result for Δ_{HHH} due to the residual tadpole contribution to the counterterm for the trilinear Higgs coupling λ_{HHH} [20].

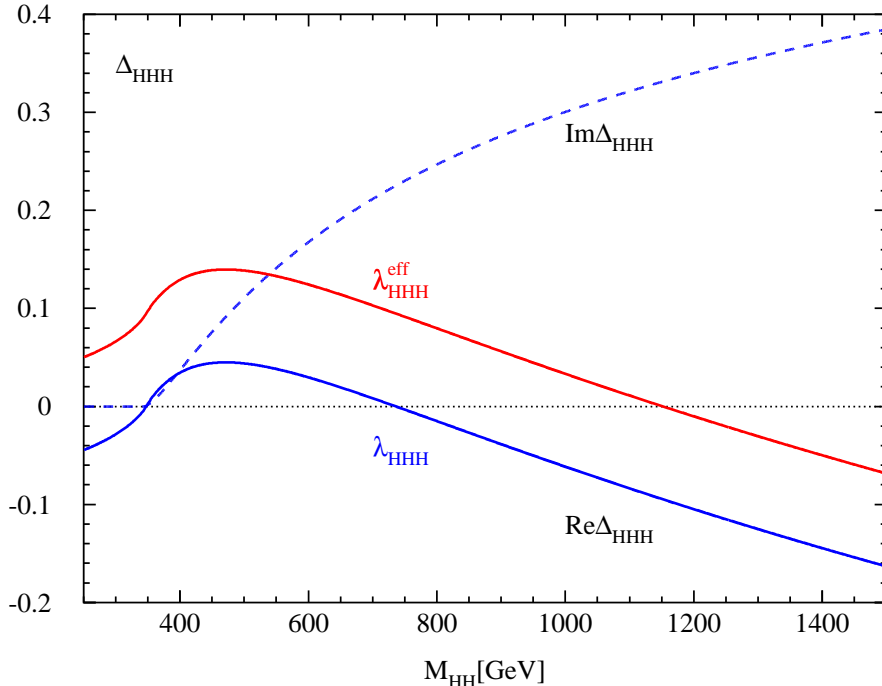


Figure 4: The relative top-Yukawa-induced electroweak correction factor Δ_{HHH} as a function of the invariant Higgs-pair mass M_{HH} . The full blue curve shows the real part of Δ_{HH} and the dashed blue on the imaginary part. The red curve exhibits the real part after introducing the effective trilinear coupling λ_{HHH}^{eff} of Eq. (16) and adding the shift of Eq. (23). To guide the eye the dotted black curve has been added as the zero-line.

[21]. The Fermi constant is chosen as $G_F = 1.1663787 \times 10^{-5} \text{ GeV}^{-2}$, the strong coupling as $\alpha_s(M_Z) = 0.118$ and the Higgs mass as $M_H = 125 \text{ GeV}$. We are using PDF4LHC15 parton densities.

The (complex) electroweak correction factor Δ_{HHH} of Eq. (20) is shown in Fig. 4 as a function of the invariant Higgs-pair mass M_{HH} . The full lines denote the real parts and the dashed line the imaginary part. The blue curves exhibit the real and imaginary parts of Δ_{HHH} in terms of the LO trilinear Higgs coupling, while the red curve shows the correction factor after introducing the effective coupling λ_{HHH}^{eff} . The size of the correction factor shows that the effective trilinear coupling does not capture the dominant part of the electroweak corrections so that its use is not supported by our results.

The relative electroweak corrections originating from the top-Yukawa-induced contributions are shown in Fig. 5 for the differential cross section as a function of the invariant Higgs-pair mass M_{HH} . The radiative corrections close to the production threshold turn out to be large. This is due to the vanishing of the matrix element in the leading term in the large inverse top-mass expansion of the LO expression of Eq. (3) so that the LO matrix element is highly suppressed at threshold. This suppression, however, is lifted by the radiative corrections to the effective trilinear Higgs coupling λ_{HHH}^{eff} or, equivalently, the mismatch of electroweak corrections to the triangle and box diagrams. However, Fig. 5 does not

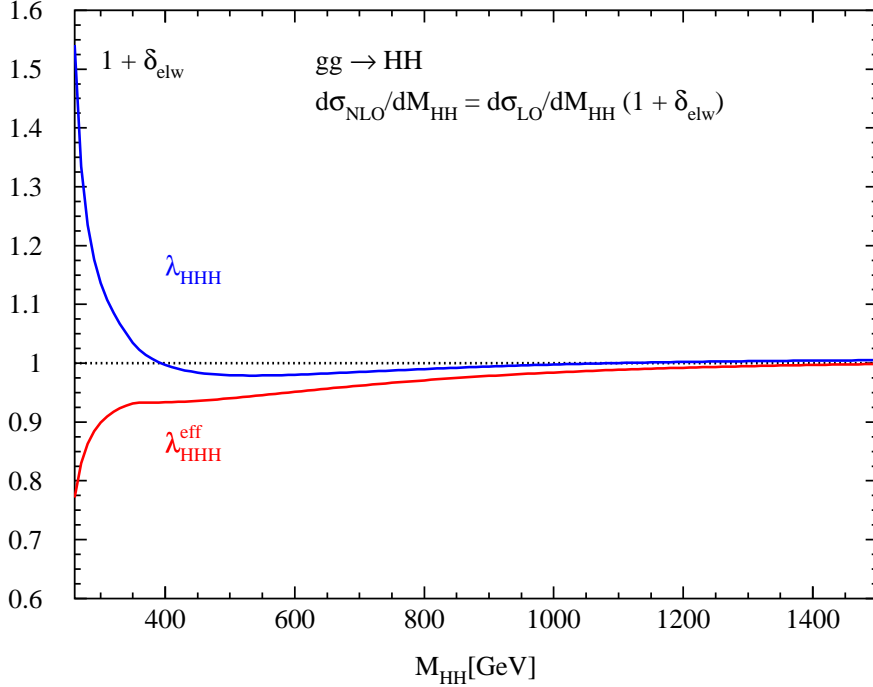


Figure 5: *The relative top-Yukawa-induced electroweak corrections to the differential Higgs-pair production cross section as a function of the invariant Higgs-pair mass M_{HH} . The blue curve shows the electroweak correction factor using the LO trilinear Higgs coupling of Eq. (5) and the red curve the corrections factor involving the effective coupling λ_{HHH}^{eff} of Eq. (16). The black dotted line at the value 1 is inserted to guide the eye. The electroweak corrections factor is independent of the hadronic c.m. energy and scale choices in the QCD part of the differential cross section $d\sigma/dM_{HH}$ so that it is valid for any hadronic energy as a pure rescaling factor.*

support the use of the effective trilinear Higgs coupling λ_{HHH}^{eff} to improve the perturbative result. Thus, the naive argument that the effective trilinear Higgs coupling induces a SM contribution to κ_λ ,

$$\begin{aligned}
 \lambda_{HHH}^{eff} &= \kappa_\lambda \lambda_{HHH} \\
 \lambda_{HHH} &= 3 \frac{M_H^2}{v} \\
 \kappa_\lambda &= 1 - \frac{m_t^4}{\pi^2 v^2 M_H^2} \approx 0.91
 \end{aligned} \tag{26}$$

is not supported by our results, but the inclusion of the complete electroweak corrections is mandatory instead. We observe that the electroweak corrections appear with opposite sign close to the threshold between the options of using the LO and the effective trilinear coupling.

The effect of the top-Yukawa-induced electroweak corrections on the total integrated

hadronic cross section amounts to

$$\begin{aligned}
\sigma &= K_{elw} \times \sigma_{LO} \\
K_{elw} &\approx 1.002 && (\lambda_{HHH}) \\
K_{elw}^{eff} &\approx 0.938 && (\lambda_{HHH}^{eff})
\end{aligned}
\tag{27}$$

so that the corrections induce an effect of about 0.2% on the total cross section, if the LO-like trilinear Higgs coupling λ_{HHH} is adopted. The bulk of these corrections *cannot* be absorbed in the effective triple Higgs coupling, but the latter option leads to an artificial increase of the relative electroweak corrections.

6 Conclusions

In this note we have investigated the electroweak corrections to Higgs-pair production via gluon fusion induced by top-quark contributions. While keeping the full top-mass dependence in the triple-Higgs vertex and self-energy corrections, we have worked in the HTL for the radiative corrections to the effective $ggH(H)$ vertices for the relative corrections. The top-Yukawa-induced NLO electroweak corrections to the total gluon-fusion cross section amount to about 0.2%. After integrating out the top-quark contributions an effective trilinear Higgs coupling can be defined in terms of the effective Higgs potential that is dressed with contributions scaling with the fourth power of the top mass. This is known already starting from the Coleman–Weinberg potential [18]. This effective trilinear Higgs coupling can be introduced in the full calculation of electroweak corrections as well and leads to a modification of the counterterms in order to remove potential double counting of corrections. However, introducing this effective coupling the remaining electroweak corrections turn out to be larger than in the case of the LO-like triple Higgs coupling.

Acknowledgments

The authors are indebted to A. Djouadi and P. Gambino for very helpful discussions. The research of M.M. is supported by the Deutsche Forschungsgemeinschaft (DFG, German Research Foundation) under grant 396021762–TRR 257. The work of J.S. is supported by the Swiss National Science Foundation (SNSF).

References

- [1] G. Aad *et al.* [ATLAS Collaboration], Phys. Lett. **B716** (2012) 1; S. Chatrchyan *et al.* [CMS Collaboration], Phys. Lett. **B716** (2012) 30.
- [2] G. Aad *et al.* [ATLAS and CMS Collaborations], JHEP **1608** (2016) 045; G. Aad *et al.* [ATLAS Collaboration], ATLAS-CONF-2019-005; A.M. Sirunyan *et al.* [CMS Collaboration], JHEP **01** (2021) 148.

- [3] J. Alcaraz et al. [ALEPH and DELPHI and L3 and OPAL and LEP Electroweak Working Group Coll.], arXiv:0712.0929 [hep-ex].
- [4] G. 't Hooft, Nucl. Phys. **B35** (1971) 167; G. 't Hooft and M.J.G. Veltman, Nucl. Phys. **B44** (1972) 189.
- [5] C.H. Llewellyn Smith, Phys. Lett. **46B** (1973) 233; J.M. Cornwall, D.N. Levin and G. Tiktopoulos, Phys. Rev. **D10** (1974) 1145 [Erratum-ibid. **D11** (1975) 972]; B.W. Lee et al., Phys. Rev. Lett. **38** (1977) 883 and Phys. Rev. **D16** (1977) 1519.
- [6] J. Baglio, A. Djouadi, R. Gröber, M.M. Mühlleitner, J. Quevillon and M. Spira, JHEP **1304** (2013) 151; B. Di Micco, M. Gouzevitch, J. Mazzitelli, C. Vernieri, J. Alison, K. Androsov, J. Baglio, E. Bagnaschi, S. Banerjee and P. Basler, *et al.*, Rev. Phys. **5** (2020) 100045.
- [7] S. Dawson, S. Dittmaier and M. Spira, Phys. Rev. **D58** (1998) 115012.
- [8] A. Djouadi, W. Kilian, M. Mühlleitner and P.M. Zerwas, Eur. Phys. J. **C10** (1999), 45.
- [9] S. Borowka et al., Phys. Rev. Lett. **117** (2016) no.1, 012001 [Erratum-ibid. **117** (2016) no.7, 079901]; S. Borowka et al., JHEP **1610** (2016) 107.
- [10] J. Baglio, F. Campanario, S. Glaus, M. Mühlleitner, M. Spira and J. Streicher, Eur. Phys. J. **C79** (2019) no.6, 459; J. Baglio, F. Campanario, S. Glaus, M. Mühlleitner, J. Ronca, M. Spira and J. Streicher, JHEP **04** (2020), 181; J. Baglio, F. Campanario, S. Glaus, M. Mühlleitner, J. Ronca and M. Spira, Phys. Rev. **D103** (2021) no.5, 056002.
- [11] D. de Florian and J. Mazzitelli, Phys. Lett. **B724** (2013) 306 and Phys. Rev. Lett. **111** (2013) 201801; J. Grigo et al., Nucl. Phys. **B888** (2014) 17; M. Grazzini, G. Heinrich, S. Jones, S. Kallweit, M. Kerner, J. M. Lindert and J. Mazzitelli, JHEP **1805** (2018) 059.
- [12] L. B. Chen, H. T. Li, H. S. Shao and J. Wang, Phys. Lett. **B803** (2020) 135292 and JHEP **2003** (2020) 072.
- [13] J. Grigo, J. Hoff and M. Steinhauser, Nucl. Phys. **B900** (2015) 412.
- [14] D.Y. Shao, C.S. Li, H.T. Li and J. Wang, JHEP **1307** (2013) 169; D. de Florian and J. Mazzitelli, JHEP **1509** (2015) 053.
- [15] E. W. N. Glover and J. J. van der Bij, Nucl. Phys. **B309** (1988) 282; T. Plehn, M. Spira and P. M. Zerwas, Nucl. Phys. **B479** (1996) 46, Erratum: [Nucl. Phys. **B531** (1998) 655].
- [16] A. Djouadi and P. Gambino, Phys. Rev. Lett. **73** (1994) 2528; K. G. Chetyrkin, B. A. Kniehl and M. Steinhauser, Nucl. Phys. **B490** (1997) 19.

- [17] B.A. Kniehl, Nucl. Phys. **B376** (1992) 3; B.A. Kniehl and M. Spira, Nucl. Phys. **B432** (1994) 39 and B. A. Kniehl and M. Spira, Z. Phys. **C69** (1995) 77; A. Kwiatkowski and M. Steinhauser, Phys. Lett. **B338** (1994) 66, Erratum: [Phys. Lett. **B342** (1995) 455].
- [18] S.R. Coleman and E.J. Weinberg, Phys. Rev. **D7** (1973) 1888; S. Weinberg, Phys. Rev. **D7** (1973) 2887; R. Jackiw, Phys. Rev. **D9** (1974) 1686.
- [19] J. Fleischer and F. Jegerlehner, Phys. Rev. **D23** (1981) 2001.
- [20] A. Denner and S. Dittmaier, Phys. Rept. **864** (2020) 1.
- [21] D. de Florian *et al.* [LHC Higgs Cross Section Working Group Collaboration], arXiv:1610.07922 [hep-ph].